Blast Behavior of One-Way Panel Components Constructed with UHPC

Author(s) & Affiliation: Christian Melançon[1], Sarah De Carufel[1] and Hassan Aoude[2]

[1]Master's Candidate, University of Ottawa

[2]Associate Professor, University of Ottawa

Abstract: This paper summarizes the results from three one-way slabs which were tested under gradually increasing shockwave loads using a high-capacity shock-tube at the University of Ottawa. The series includes one control slab built with conventional concrete and two companion slabs built with ultra-high performance concrete (UHPC). Results in terms of blast resistance, control of displacements, and damage tolerance are used to study the effects of the design parameters on the performance of the panels. Overall, the results demonstrate significant benefits associated with the use of UHPC in reinforced concrete slabs tested under extreme blast pressures.

Keywords: UHPC, high-strength steel, shockwave loading, blast resistance, slabs.

1. Introduction

The superior compressive strength, tensile resistance and toughness of ultra-high performance concrete (UHPC) make this class of material ideally-suited for the mitigation of blast hazards on critical infrastructure. However, research data is required in order to successfully adapt this innovative material in the blast-resistant design of concrete structures. This paper summarizes the results from an ongoing research project examining the performance enhancements that can be achieved by using high-performance materials in reinforced concrete structural members subjected to extreme blast loads. As part of the study, a series of three one-way slabs were tested under simulated blast loading using a high-capacity shock-tube at the University of Ottawa. The series includes one control slab built with conventional concrete and two companion slabs built with UHPC. Results in terms of blast resistance, control of displacements, and damage tolerance are used to study the effects of the test parameters on the blast performance of the panels.

2. Background

2.1. Compact Reinforced Composite (CRC)

Compact reinforced composite (CRC) was developed by Aalborg Portland A/S in Denmark and patented in 1986. It is a type of ultra-high performance concrete with the capabilities to achieve high compressive strength, the result of a combination of low water-binder ratio (approximately 0.18), Densit Binder (cement and microsilica), the lack of coarse aggregates, quartz sand and dense particle packing (Aarup, 1998). With the addition of steel fibers, usually between 2% and 6% of the concrete volume, CRC exhibits improved tensile resistance, toughness, ductility and damage control comparatively to conventional concrete. A number of research studies have been conducted to demonstrate the potential of using CRC in heavily-loaded structural members (Aarup, 1998). The enhanced properties of CRC could also make it well-suited for extreme load applications.

2.2. Previous Research on the Blast Performance of UHPC Panels

A limited number of studies have been conducted on UHPC slabs and panels subjected to blast loads. Cavill et al. (2006) conducted live tests on seven unreinforced pre-stressed and non-pre-stressed Ductal panels located at different far-range standoff distances from the explosives. Compared with conventional concrete panels, Ductal panels exhibited improved ductility and no signs of fragmentation. Pre-stressed panels were capable of absorbing greater amounts of energy from the blast without showing fractures, significant residual displacements or excessive fragmentation. Additional Ductal panels were tested at far-range standoff distances by Ngo et al. (2007), and at close range by Wu et al. (2007) with similar observations. As for simulated blast tests, Ellis et al. (2014) conducted experiments on four simply-supported unreinforced UHPC panels using a blast load simulator. Following the validation of a multiscale model, a parametric study showed that steel fiber properties such as volume ratio, aspect ratio and fiber packing have an important effect on increasing energy dissipation when using UHPC.

3. Testing Methods

3.1. Details of the Test Specimens

A total of three reinforced concrete one-way panels were tested as part of this study. The series included one control slab built with normal-strength self-consolidating concrete (SCC) and ordinary steel, and two companion specimens built with CRC, and either ordinary (NS) or high-strength (HS) steel. As shown in Figure 1, the one-way slabs had a depth of 100 mm, a width of 400 mm and a length of 2440 mm (4 × 16 × 96 in). The longitudinal reinforcement consisted of four top and four bottom #3 bars (diameter = 9.5 mm (0.4 in), area = 71 mm^2 (0.11 in^2)) with 180° extensions. The cover was 6 mm (0.2 in) in all slabs. Table 1 summarizes the properties of the specimens and provides information regarding concrete type (SCC/CRC), fiber content (0-2%) and steel reinforcement type (NS or HS).

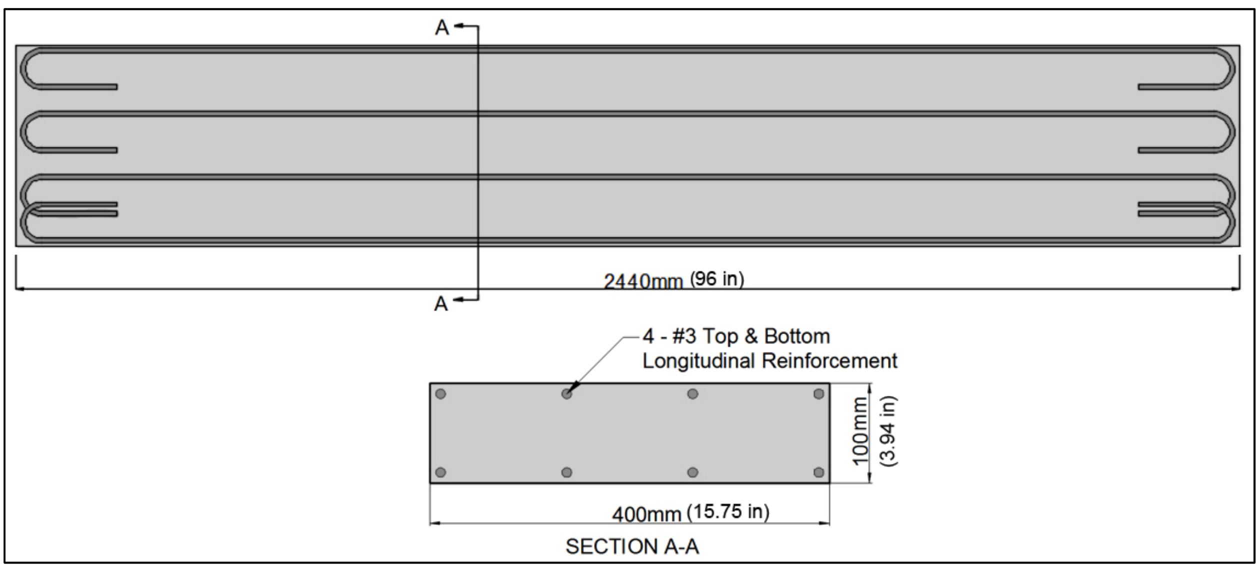

Figure 1: Specimens geometry

Table 1: Properties of specimens tested in the experimental program

Specimen ID	Concrete Type	Fiber Content	Steel Type	Compressive strength (MPa)
SCC-0%-#3NS	SCC	0%	NS	61.3
CRC-2%A-#3NS	CRC	2%	NS	149.6
CRC-2%A-#3HS	CRC	2%	HS	146.5

3.2. Material Parameters

The control slab was cast using plain self-consolidating concrete (SCC) with a specified strength of 50 MPa (5.8 ksi). The SCC mix properties include a maximum aggregate size of 10 mm (0.4 in), a sand-to-aggregate ratio of 0.55 and a water-cement ratio of approximately 0.42 (Burrell et al., 2015). The UHPC specimens were cast using compact reinforced composite (CRC) with a specified strength of 140 MPa (20 ksi). Straight steel fibers were incorporated into the CRC mix for additional tensile resistance, ductility and toughness. The fibers had a length of 13 mm (0.5 in), an aspect-ratio (length/diameter) of 62, with a tensile strength of 2750 MPa (400 ksi), and were added at volumetric ratio of 2%. Figure 2a shows the typical stress-strain curves for SCC and CRC obtained from testing cylinders having diameter of 100 mm (4 in) and height of 200 mm (8 in), with average compressive strengths reported in Table 1.

Two types of #3 bars were used in this study. The ordinary steel bars (NS) had yield strength of 435 MPa (63 ksi), ultimate tensile strength of 625 MPa (91 ksi), while the high-strength steel bars (HS) were made of a corrosion-resistant low-carbon chromium-steel alloy, with a strength at yielding/at failure in tension close to 1000/1200 MPa (145/174 ksi) (MMFX Corporation of America, 2013). Typical stress-strain curves in tension are shown in Figure 2b for both regular and high-strength steel bars.

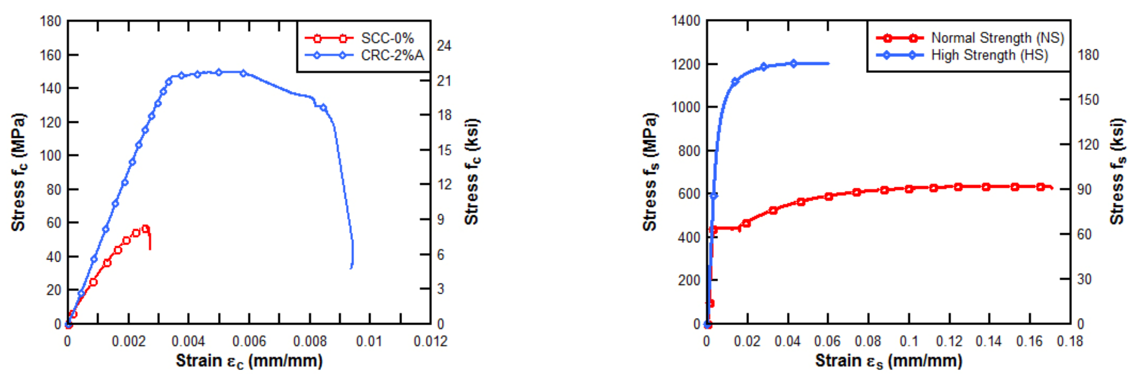

(a) Concrete in compression (b) Steel reinforcement in tension

Figure 2: Stress-strain curves for concrete in compression and steel in tension

3.3. Instrumentation and Setup

The slab specimens were tested under simulated blasting using a high-capacity shock-tube at the University of Ottawa. As illustrated in Figure 3, the shock-tube is divided into three sections: the variable length driver section which generates the shockwave, the spool section which controls the release of the shockwave using a double differential pressure diaphragm, an expansion section which expands to the test frame (Lloyd et al. 2011). A load transfer device (LTD) as shown on Figure 3 was used to redirect the positive phase of the blast as an uniformly distributed load onto the specimens. The boundary conditions for the slabs corresponded to simple-support conditions. The instrumentation included piezoelectric pressure sensors, two linear variable displacement transducers (LVDT) located at mid and one-third height of the specimens (see Figure 3), as well as a high-speed video camera.

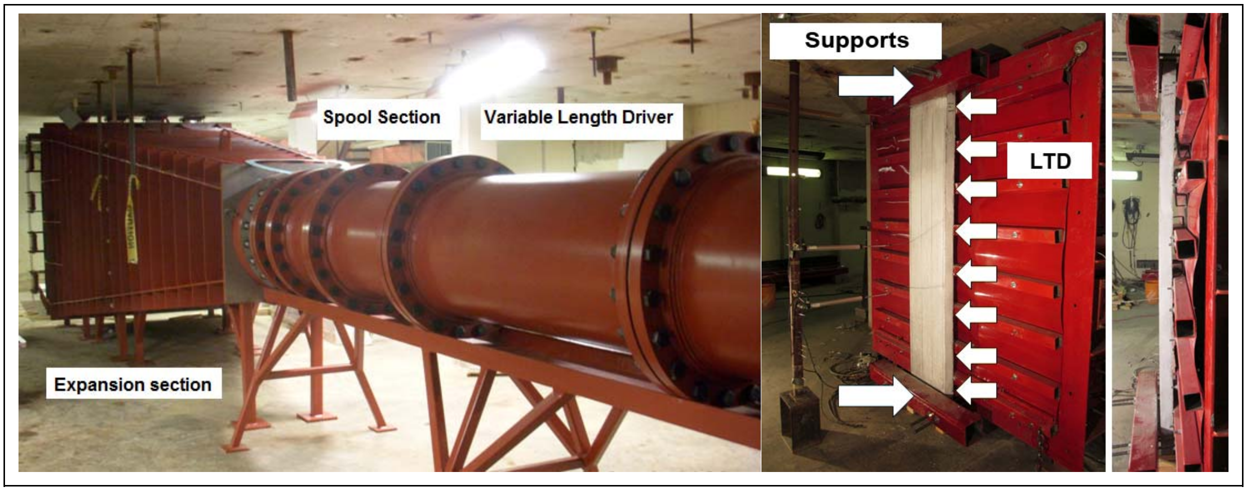

Figure 3: University of Ottawa shock-tube & load transfer device for slabs

3.4. Experimental Procedures

Each specimen was subjected to gradually increasing blast loads until failure. The shock-tube driver length was kept constant at 1830 mm (6 ft), while the driver pressures were increments of 103 kPa (15 psi). The magnitude of the reflected pressure ranged between 16.5 kPa (2.4 psi-ms) for the initial blast 1 to 87.2 kPa (12.6 psi-ms) for blast 6. Reflected impulse ranged between 131 kPa-ms (19.0 psi-ms) to 535 kPa-ms (77.6 psi-ms). A sample of pressure-time histories for each blast test is included in Figure 4 while shockwave data for each specimen can be found in Table 2. The initial blast test was meant to be within the elastic range of specimen's behavior, while the remaining blasts aimed at gradually increasing damage and continued until specimen failure.

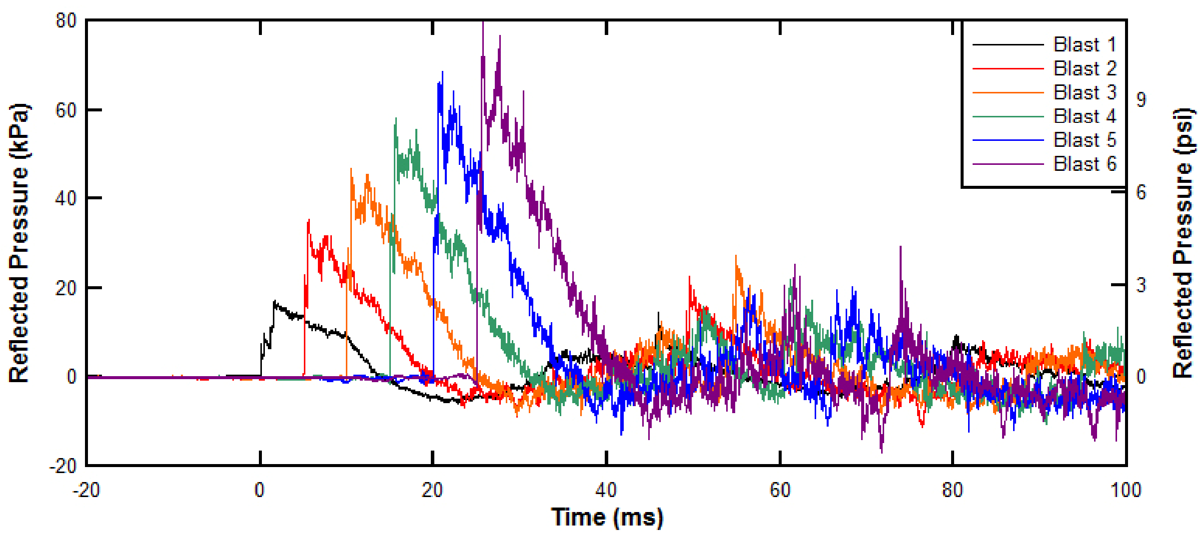

Figure 4: Sample pressure-time histories from specimen CRC-2%A-#3HS

Table 2: Shockwave properties for slab specimens

Specimen	Shockwave Properties	Blast 1	Blast 2	Blast 3	Blast 4	Blast 5	Blast 6
SCC-0%-#3NS	Reflected Pressure, P_r (kPa)	18.9	34.6	45.3	53.2	No Data	-
	Reflected Impulse, I_r (kPa-ms)	138	238	319	351	No Data	-
CRC-2%A-#3NS	Reflected Pressure, P_r (kPa)	16.5	39.5	47.4	56.5	67.4	-
	Reflected Impulse, I_r (kPa-ms)	131	267	323	365	440	-
CRC-2%A-#3HS	Reflected Pressure, P_r (kPa)	17.3	35.4	46.7	58.3	68.5	87.2
	Reflected Impulse, I_r (kPa-ms)	134	243	350	421	469	535

4. Results

Table 2 reports the experimental results from the research program in terms of maximum mid-height displacements (**δ_{max}**) and residual mid-height displacements (**$\delta_{residual}$**) for each blast test. Post-blast test photographs are shown in Figure 5.

Table 3: Experimental results for slab specimens

Specimen	Displacements*	Test #					
		Blast 1	Blast 2	Blast 3	Blast 4	Blast 5	Blast 6
SCC-0%-#3NS	δ_{max} (mm)	23.5	52.8	84.9	110.2	No Data	-
	$\delta_{residual}$ (mm)	7.1	29.3	46.3	58.1	No Data	-
CRC-2%A-#3NS	δ_{max} (mm)	12.1	33.9	49.7	67.3	213.1	-
	$\delta_{residual}$ (mm)	3.3	12.4	19.3	38.4	137.3	-
CRC-2%A-#3HS	δ_{max} (mm)	13.0	27.8	45.1	59.4	71.9	128.5
	$\delta_{residual}$ (mm)	2.5	2.0	6.5	12.1	14.7	66.5

*Note: 1 mm = 0.0394 in

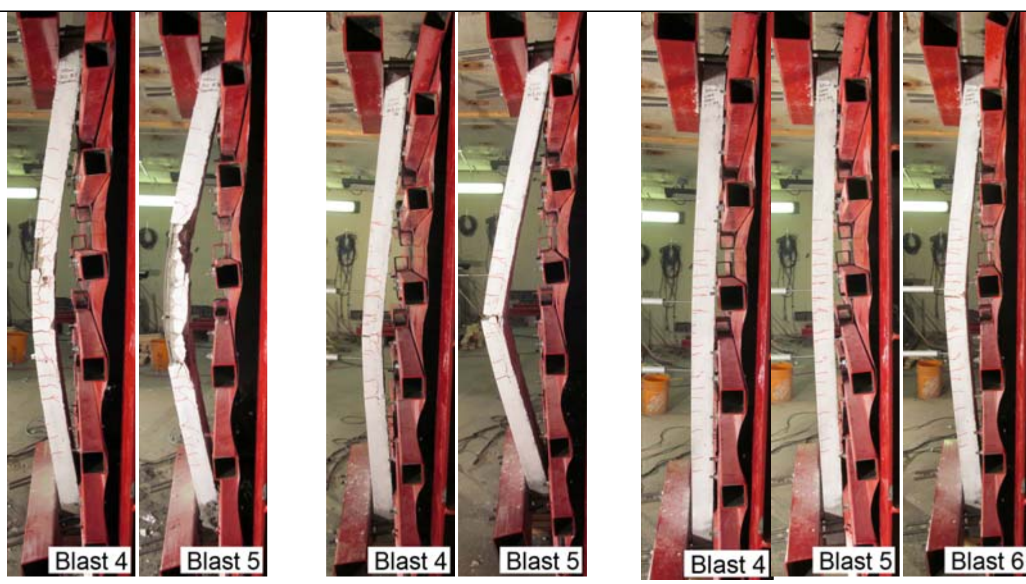

(a) SCC-0%-#3NS (b) CRC-2%A-#3NS (c) CRC-2%A-#3HS

Figure 5: Typical cases of cracking and failure for slab specimens subjected to blasts 4-6

5. Discussion

5.1. Effect of UHPC on Slab Performance

Comparisons between the behavior of the control slab (SCC-0%-#3NS) and the companion CRC slab with conventional steel (CRC-2%A-#3NS) demonstrate significant improvements regarding the use of UHPC in slabs. For instance, during blast 3, the CRC specimen exhibited improved control of lateral displacements by effectively reducing the maximum deflection by 41% and the residual deflection by 58% when compared to the control specimen. During blast 4, the maximum and residual displacements of the control specimen were 110.2 mm (4.34 in) and 58.1 mm (2.29 in) respectively against 67.3 mm (2.65 in) and 38.4 mm (1.51 in) for CRC-2%A-#3NS (see Figure 7a). The CRC specimen decreased the maximum deflection by 39% and the permanent deformation by 34% when compared to the control specimen. This trend could be observed throughout the testing phase (refer to Table 2).

Furthermore, UHPC enhanced the control of tensile cracking (see Figure 5a vs. Figure 5b) and zeroed secondary fragmentation (see Figure 6a vs. Figure 6b). However, the greater strength of CRC lead to the brittle failure of specimen CRC-2%A-#3NS due to the rupture of tension bars under blast 5.

(a) SCC-0%-#3NS (b) CRC-2%A-#3NS (c) CRC-2%A-#3HS

Figure 6: Secondary fragmentation during blast 5

5.2. Effect of Combined Use of UHPC and High-Strength Steel Reinforcement

The test results from Table 2 show that using high-strength steel reinforcement further improves the behavior of concrete slabs. When comparing specimens CRC-2%A-#3NS and CRC-2%A-#3HS, it was observed that the introduction of high-strength reinforcement in UHPC slabs (CRC-2%A-#3HS) resulted in significant reductions in both maximum and permanent deflections, such as demonstrated in Table 2 and Figure 7. For instance, the maximum and residual displacements of the high strength steel specimen CRC-2%A-#3HS during and after blast 4 were 59.4 mm (2.34 in) and 12.1 mm (0.48 in) respectively against 67.3 mm (2.65 in) and 38.4 mm (1.51 in) for the conventional steel specimen CRC-2%A-#3NS, effectively reducing both types of deformations for this event by 11% and 68% (see Figure 7a). Likewise, this trend was observed throughout the testing phase (see Table 2 and Figure 7b).

In addition, these enhancements to the behavior of the reinforced concrete slab are noted along with less tensile cracking (see Figure 5c) at equivalent blasts with no significant fragmentation (see Figure 6c). The combined use of CRC and high-strength steel also allowed the companion slab CRC-2%A-#3HS to resist larger blast loads (see Figure 7b), although the specimen ultimately failed due to the rupture of tension bars during blast 6.

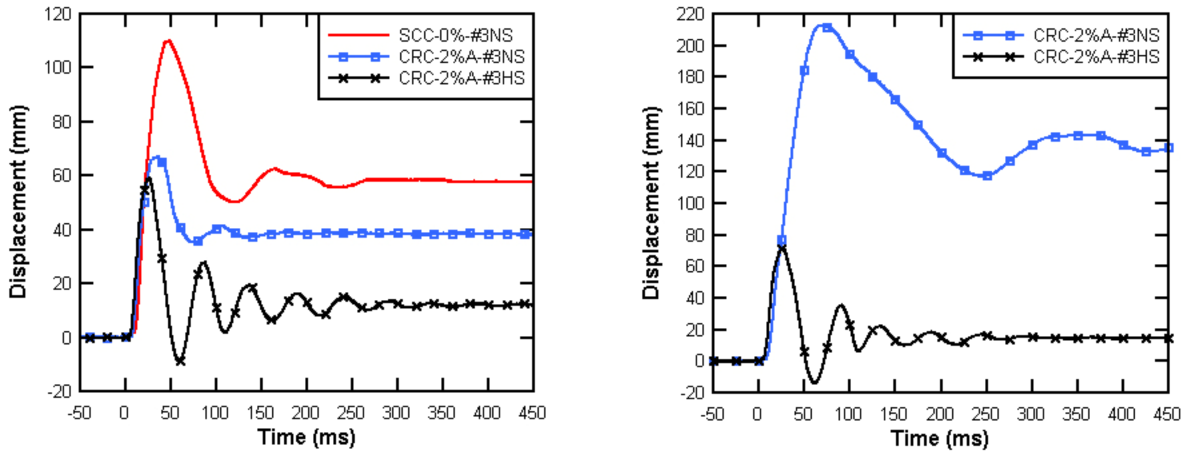

(a) Slab mid-height displacements - Blast 4 (b) Slab mid-height displacements - Blast 5

Figure 7: Maximum and residual displacements for slabs at selected blast tests

*Note: 1 mm = 0.0394 in

6. Conclusions

The paper presented the results from three one-way panels tested under simulated blast loads using a shock-tube. The series included one control specimen built with conventional concrete and two UHPC specimens built with ordinary and high-strength steel reinforcement. The following conclusions are drawn from this study:

- The results demonstrate that using UHPC in slabs improves blast performance by reducing maximum and residual displacements under equivalent blast loads;
- The results demonstrate that using UHPC enhances damage tolerance, by improving the control of tensile cracking and minimizing secondary fragmentation in slabs subjected to blast loads;
- The combined use of UHPC and high-strength steel reinforcement leads to further enhancements in the blast performance of slabs and results in reduced displacements at equivalent blasts and increased blast capacity.

7. References

Aarup, B., "Fiber Reinforced High Performance Concrete for Precast Applications." *Proc. International Symposium on High Performance and Reactive Powder Concretes, Sherbrooke*, 1998, pp.113-123.

Burrell, R. P., Aoude, H. and Saatcioglu, M.: Response of SFRC Columns under Blast Loads." *ASCE Journal of Structural Engineering 141 (9)*, 2015, pp. 1-18.

Cavill, B., Rebentrost, M. and Perry, V., "Ductal – An ultra-high performance material for resistance to blasts and impacts." *Proc. 1st Specialty Conf. on Disaster Mitigation, Calgary, Canada*, 2006, pp.1-10.

Ellis, B. D., DiPaolo, B. P., McDowell, D. L. and Zhou, M., "Experimental investigation and multiscale modeling of ultra-high performance concrete panels subjected to blast loading." *International Journal of Impact Engineering 69*, 2014, pp.95-103.

Lloyd, A., Jacques, E., Saatcioglu, M., Palermo, D., Nistor, I. and Tikka, T., "Capabilities of a Shock Tube to Simulate Blast Loading on Structures." *ACI Special Publication SP-281-3*, 2011, pp.1-20.

MMFX Steel Corporation of America, "MMFX2 Rebar–Product Guide Specification." Available at www.mmfx.com/wp-content/uploads/2013/10/Product_Guide_Specification_Sept2013.pdf. [Cited February 1, 2016].

Ngo, T., Mendis, P. and Krauthammer, T., "Behaviour of ultrahigh-strength prestressed concrete panels subjected to blast loading." *Journal of Structural Engineering 133 (11),* 2007, pp. 1582-1590.

Wu,C., Oehlers, D. J., Rebentrost, M., Leach, J. and Whittaker, A. S., "Blast testing of ultra-high performance fibre and FRP reinforced concrete slabs." *Engineering Structures 31 (9)*, 2007, pp.2060-2069.

8. Acknowledgements

The authors would like to thank CRC Technology (Hi-Con A/S) and MMFX Technologies Corporation for providing the materials used in this study.